

Developing a Linear Fluid Plasma Model with Accurate Kinetic Bernstein Waves: A First Step

Huasheng Xie^{1,2,*}

¹Hebei Key Laboratory of Compact Fusion, Langfang 065001, China

²ENN Science and Technology Development Co., Ltd., Langfang 065001, China

(Dated: February 11, 2025)

Kinetic models provide highly accurate descriptions of plasma waves but involve complex integrals that are computationally expensive to solve. To facilitate a fluid-like treatment of the system, we propose rational approximations for both the plasma dispersion function in the parallel integral and the Bessel function in the perpendicular integral, ensuring that the system remains rational with respect to all three variables: wave frequency ω , parallel wavevector k_{\parallel} , and perpendicular wavevector k_{\perp} . By accurately approximating the Bessel function over a wide range of Larmor radius ρ_{cs} values, from $k_{\perp}\rho_{cs} \rightarrow 0$ to $k_{\perp}\rho_{cs} \rightarrow \infty$, we present an initial attempt to incorporate kinetic Bernstein waves into a fluid model. As an application, we employ this model to analyze wave propagation conditions (i.e., accessibility) by solving for the complex perpendicular wavevector k_{\perp} using a matrix eigenvalue method with given input parameters. This work may contribute to studies of electron cyclotron resonance heating (ECRH) and ion cyclotron resonance frequency (ICRF) heating in magnetized confinement plasmas.

We consider local linear kinetic plasma waves in an infinite, homogeneous system with a Maxwellian velocity distribution for each species, given by $f_{s0} = \pi^{-3/2} v_{ts}^{-3} \exp[-(v_{\parallel}^2 + v_{\perp}^2)/v_{ts}^2]$. The background magnetic field is assumed to be $\mathbf{B}_0 = (0, 0, B_0)$, and the wave vector is given by $\mathbf{k} = (k_x, 0, k_z) = (k \sin \theta, 0, k \cos \theta)$, such that $k_{\parallel} = k_z$ and $k_{\perp} = k_x$. We consider S species, indexed by $s = 1, 2, \dots, S$. The electric charge, mass, density, and temperature of each species are denoted as q_s , m_s , n_{s0} , and T_{s0} , respectively. The thermal velocity is defined as $v_{ts} = \sqrt{\frac{2k_B T_{s0}}{m_s}}$ (some authors may use $v_{ts} = \sqrt{\frac{k_B T_{s0}}{m_s}}$), where k_B is the Boltzmann constant.

The non-relativistic kinetic dispersion relation (KDR) is

$$D(\omega, \mathbf{k}) = |\mathbf{K}(\omega, \mathbf{k}) + (\mathbf{k}\mathbf{k} - k^2\mathbf{I})\frac{c^2}{\omega^2}| = 0, \quad (1)$$

where

$$\mathbf{K} = \mathbf{I} + \mathbf{Q} = \mathbf{I} - \frac{\boldsymbol{\sigma}}{i\omega\epsilon_0}, \quad \mathbf{Q} = -\frac{\boldsymbol{\sigma}}{i\omega\epsilon_0}. \quad (2)$$

Define $a_s = k_{\perp}\rho_{cs}$, $b_s = a_s^2 = k_{\perp}^2\rho_{cs}^2$, $\rho_{cs} = v_{ts}/(\sqrt{2}\omega_{cs})$, $\mathbf{n} = \mathbf{k}c/\omega$, $\omega_{cs} = q_s B_0/m_s$, $\omega_{ps} = \sqrt{n_{s0}q_s^2/(\epsilon_0 m_s)}$, $c = 1/\sqrt{\mu_0\epsilon_0}$ and $\zeta_{sn} = (\omega - n\omega_{cs})/(k_z v_{ts})$, where c is the speed of light, ω_{ps} and ω_{cs} are the plasma frequency and cyclotron frequency of each species, ϵ_0 is the permittivity of free space, and μ_0 is the permeability of free space. Note that for electrons, $q_s < 0$, and thus ω_{cs} , ρ_{cs} , and a_s are negative. After standard derivations [1–3], we obtain

$$\mathbf{K} = \mathbf{I} + \sum_s \frac{\omega_{ps}^2}{\omega^2} \left[\sum_{n=-\infty}^{\infty} \zeta_{s0} Z(\zeta_{sn}) \mathbf{X}_{sn} + 2\zeta_{s0}^2 \hat{\mathbf{z}}\hat{\mathbf{z}} \right], \quad (3)$$

and

$$\mathbf{X}_{sn} = \begin{bmatrix} \frac{n^2}{b_s} \Gamma_{sn} & in\Gamma'_{sn} & \sqrt{2}\zeta_{sn} \frac{n}{a_s} \Gamma_{sn} \\ -in\Gamma'_{sn} & \frac{n^2}{b_s} \Gamma_{sn} - 2b_s \Gamma'_{sn} & -i\sqrt{2}\zeta_{sn} a_s \Gamma'_{sn} \\ \sqrt{2}\zeta_{sn} \frac{n}{a_s} \Gamma_{sn} & i\sqrt{2}\zeta_{sn} a_s \Gamma'_{sn} & 2\zeta_{sn}^2 \Gamma_{sn} \end{bmatrix},$$

where $Z(\zeta) = \frac{1}{\sqrt{\pi}} \int_{-\infty}^{+\infty} \frac{e^{-z^2}}{z-\zeta} dz$ is the plasma dispersion function[4], $\Gamma_{sn} \equiv \Gamma_n(b_s)$ and $\Gamma'_{sn} \equiv \Gamma'_n(b_s)$, with $\Gamma_n(b) = I_n(b)e^{-b}$, $\Gamma'_n(b) = (I'_n - I_n)e^{-b}$, $I'_n(b) = (I_{n+1} + I_{n-1})/2$, $I_{-n} = I_n$, $Z'(\zeta) = -2[1 + \zeta Z(\zeta)]$, and I_n is the n -th order modified Bessel function. Note also the symmetry relations $K_{yx} = K_{xy}$, $K_{zx} = K_{xz}$ and $K_{zy} = -K_{yz}$.

Due to the complexity of the plasma dispersion function $Z(\zeta)$ and the infinite-order summation of Γ_n , the KDR takes a complicated form in terms of ω , k_z , and k_x . In particular, the integral form of $Z(\zeta)$ makes computations expensive. The search for a fluid model that can effectively mimic both the kinetic Landau damping effects from $Z(\zeta)$ and the finite Larmor radius (FLR) effects from the zeroth-order Bessel function term $\Gamma_0(b)$ has led to the widely used gyro-Landau-fluid model [5–7]. However, while the gyro-Landau-fluid model is mainly used for nonlinear and non-uniform studies, it provides only a rough approximation of kinetic effects and is valid only for low-frequency waves, where $\omega \ll \omega_{ci}$.

We are interested in capturing linear kinetic effects accurately within a fluid model, which is crucial for studying plasma waves. By a "fluid model", we mean a system that takes a simple algebraic form in terms of ω , k_z , and k_x , or equivalently, in terms of $\partial/\partial t$, ∇_{\parallel} , and ∇_{\perp} . This is achievable if we construct accurate rational approximations for $Z(\zeta)$ and $\Gamma_n(b)$ using a finite number of terms.

In the cold plasma limit or only for lowest order FLR effects, the approximations $\zeta \rightarrow \infty$ and $b \rightarrow 0$ are often used to simplify the model. However, we aim to construct a fluid model that remains valid across all ranges of ζ

*Email: huashengxie@gmail.com, xiehuasheng@enn.cn

(which depends on ω and k_z) and b (which depends on k_x).

As a first step, we seek to construct an equivalent fluid model that accurately captures the major physical solutions of the KDR given by Eq. (1). This is achieved through highly accurate rational approximations of $Z(\zeta)$ and $\Gamma_n(b)$, followed by a linear transformation into a matrix form. We present the details of this approach in this work.

The function $Z(\zeta)$ has been approximated with high accuracy using Padé approximations and J-pole expansions [4, 8, 9], expressed as $Z(\zeta) \simeq \sum_{j=1}^J \frac{b_j}{\zeta - c_j}$, where even for $J = 8$, the error is less than 10^{-6} . This method has been successfully applied to obtain all solutions of the KDR for ω using a matrix method [3, 10], which remains valid for all significant solutions except for strongly damped modes, which are typically of lesser interest.

The accurate rational approximation of $\Gamma_n(b_s)$ is slightly complicated. For ion cyclotron resonance frequency (ICRF) studies, a Taylor expansion up to $\mathcal{O}(b_s)$ is commonly used [11]. Additionally, a fitting approach using a truncated polynomial [12, 13] has been applied for $b_s > 1$. However, this method remains invalid as $b_s \rightarrow \infty$. Since our goal is to provide a rational form for all ω , k_z , and k_x in Eq. (1), the formulation by Rönmark [9] serves as a suitable starting point, where the plasma dispersion function $Z(\zeta)$ is already expressed in a rational form. In this approach, the term \mathbf{Q} in the KDR is modified to

$$\mathbf{Q} = \sum_s \frac{\omega_{ps}^2}{\omega \omega_{cs}} \sum_j b_j \cdot \begin{bmatrix} R_{sj} & \frac{i}{x_{sj}} R'_{sj} & \frac{\sqrt{2} a_s c_j}{x_{sj}} R_{sj} \\ -\frac{i}{x_{sj}} R'_{sj} & R_{sj} - \frac{2b_s}{x_{sj}^2} R'_{sj} & -\frac{i\sqrt{2} a_s c_j}{x_{sj}^2} R'_{sj} \\ \frac{\sqrt{2} a_s c_j}{x_{sj}} R_{sj} & \frac{i\sqrt{2} a_s c_j}{x_{sj}^2} R'_{sj} & \frac{2c_j^2}{x_{sj}^2} (x_{sj} + b_s R_{sj}) \end{bmatrix}, \quad (4)$$

where b_j and c_j are Padé approximation coefficients [4, 8] for the $Z(\zeta)$ function, and $x_{sj} = (\omega - k_z v_{ts} c_j) / \omega_{cs}$ with $R_{sj} = R(x_{sj}, b_s)$. Here

$$R(x, \lambda) \equiv \sum_{n=-\infty}^{\infty} \frac{n^2 \Gamma_n(\lambda)}{\lambda(x-n)} = -\frac{x}{\lambda} + x^2 \sum_{n=-\infty}^{\infty} \frac{\Gamma_n(\lambda)}{\lambda(x-n)}, \quad (5)$$

$$R'(x, \lambda) \equiv \frac{\partial[\lambda R(x, \lambda)]}{\partial \lambda} = \sum_{n=-\infty}^{\infty} \frac{n^2 \Gamma'_n(\lambda)}{(x-n)} = x^2 \sum_{n=-\infty}^{\infty} \frac{\Gamma'_n(\lambda)}{(x-n)}, \quad (6)$$

where $\sum_{n=-\infty}^{\infty} \Gamma_n(b) = 1$, $\sum_{n=-\infty}^{\infty} n \Gamma_n(b) = 0$ and $\sum_{n=-\infty}^{\infty} n^2 \Gamma_n(b) = b$. There are two approaches to computing $R(x, \lambda)$. One method is to truncate the summation over n to a finite N , which may be inaccurate for larger λ . Alternatively, a more precise approach is to use methods that account for all n , such as those discussed in [8, 14], ensuring accuracy for all values of λ .

In this work, we fit $\Gamma_n(b)$ by truncating the summation $\sum_{n=-\infty}^{\infty}$ to $\sum_{n=-N}^N$. Considering that for large b [15], we

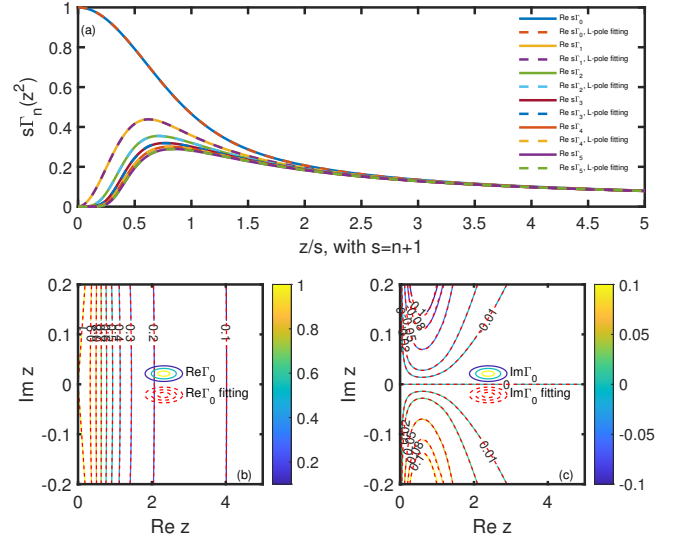


FIG. 1: The comparison of L-pole fitting for $\Gamma_n(z^2)$ demonstrates excellent agreement for both the real and imaginary parts, even for $\text{Im}(z) = 0.2$.

have

$$\Gamma_n(b) = \frac{1}{\sqrt{2\pi b}} \left[1 - \frac{(4n^2 - 1)}{8b} + \frac{(4n^2 - 1)(4n^2 - 9)}{2!(8b)^2} - \dots \right], \quad |\arg b| < \frac{\pi}{2},$$

and for small b ,

$$\Gamma_n(b) = e^{-b} \sum_{m=0}^{\infty} \frac{1}{m! \Gamma(m+n+1)} \left(\frac{b}{2} \right)^{2m+n}, \quad (7)$$

with the expansion $e^{-b} = 1 - b + \frac{b^2}{2!} - \dots$, where Γ denotes the Euler gamma function. To approximate $\Gamma_n(b)$ in a rational form, we use an L -pole expansion ($n \geq 0$),

$$\Gamma_n(z^2) = \frac{z^{2n} (a_0 + a_2 z^2 + \dots + a_{L-1} z^{L-1})}{1 + \sqrt{2\pi} a_{L-1} z^{2n+L}} = \sum_{l_n=1}^{2n+L} \frac{r_{l_n}}{z - p_{l_n}}. \quad (8)$$

This form avoids singularities for $z > 0$ along the real axis and ensures the asymptotic behavior $\Gamma_n(z^2 \rightarrow \infty) \simeq 1/(\sqrt{2\pi} z)$. Additionally, we note that $\Gamma_{-n} = \Gamma_n$. To prevent unphysical solutions in Eq. (4), we enforce constraints up to $O(z^3)$ and $O(1/z^3)$. Specifically, for all n , we impose $a_{L-2} = 0$, $a_{L-3} = -\frac{(4n^2-1)a_{L-1}}{8}$. For $n \leq 3$, we set $a_0 = \frac{1}{\Gamma(n+1)}$, and for $n = 0$, we further impose $a_2 = -a_0$. Equation (8) is valid for $\text{Re}(z) \geq 0$, i.e., $\text{Re}(k_x \rho_{cs}) \geq 0$. Thus, in practical computations, we select only solutions with $\text{Re}(k_x) \geq 0$ and set $z = k_x |\rho_{cs}|$ in Eq. (8). Similar to the J -pole expansion of the Z function [4, 8], it follows that $\sum_{l_n} r_{l_n} p_{l_n}^0 = 1/\sqrt{2\pi}$, $\sum_{l_n} r_{l_n} p_{l_n}^1 = 0$ and $\sum_{l_n} r_{l_n} p_{l_n}^2 = -(4n^2 - 1)/(8\sqrt{2\pi})$. Additionally, we have $\sum_{l_n} r_{l_n}/p_{l_n} = 0$ ($n \geq 1$) or 1 ($n = 0$), and $\sum_{l_n} r_{l_n} p_{l_n}^2 = 0$.

Under the enforced constraints on the coefficients a_{l_n} ($l_n = 0, 2, \dots, a_{L-1}$), they are determined using least-squares fitting over the range $x \in [-0.5, 10] \times (n+1)$. To maintain an error below 1%, we require approximately $L \simeq 20$ for $n \geq 10$. For $n = 0$, $L = 12$ is sufficient to achieve high accuracy, while for $n = 1$ to 3, $L = 16$ is adequate. Fitting up to $n \leq 10$ is sufficient for most applications in electron cyclotron resonance heating (ECRH) and ion cyclotron range of frequencies (ICRF) studies. Since the analytical properties of Γ_n are preserved for both small and large z , and the fitting equation remains in a single analytic form with good continuity properties, it is also valid for weakly imaginary z . This feature is crucial for wave absorption studies.

Figure 1 shows a comparison between the fitted Γ_n and the exact values, demonstrating good agreement for both the real and imaginary parts. A set of typical coefficients for Γ_0 with $L = 12$ is: $r_{2l} = [0.2944 + 0.2999i, -0.3171 + 0.1391i, -0.3533 - 0.06956i, 0.5887 - 0.462i, -0.01285 + 0.04219i, -0.0003267 - 0.0004249i]$, $p_{2l} = [-1.2 + 0.3215i, -0.8784 + 0.8784i, 0.3215 + 1.2i, -0.3215 + 1.2i, 0.8784 + 0.8784i, 1.2 + 0.3215i]$, where the remaining terms satisfy $p_{2l-1} = p_{2l}^*$ and $r_{2l-1} = r_{2l}^*$, with * denoting complex conjugation.

Similar to the derivation of the matrix method for solving ω in the KDR [3, 10] and for k_x in the multi-fluid model [16, 17], we require only Maxwell's equations along with a relation between the perturbed current $\delta\mathbf{J}$ and the perturbed electric field $\delta\mathbf{E}$, given by $\delta\mathbf{J} = \boldsymbol{\sigma} \cdot \delta\mathbf{E}$. Maxwell's equations can then be written as

$$k_x \delta E_y = \omega \delta B_z, \quad (9a)$$

$$k_x \delta E_z = \left(\frac{k_z^2 c^2}{\omega} - \omega \right) \delta B_y - \frac{ik_z}{\omega \epsilon_0} \delta J_x, \quad (9b)$$

$$k_x \delta B_y = -\frac{\omega}{c^2} \delta E_z - \frac{i}{c^2 \epsilon_0} \delta J_z, \quad (9c)$$

$$k_x \delta B_z = \left(\frac{\omega}{c^2} - \frac{k_z^2}{\omega} \right) \delta E_y + \frac{i}{c^2 \epsilon_0} \delta J_y, \quad (9d)$$

and $\delta E_x = (k_z c^2 / \omega) \delta B_y - i \delta J_x / (\omega \epsilon_0)$ and $\delta B_x = -(k_z / \omega) \delta E_y$. It can be shown that after the L-pole rational expansion of Γ_n , we obtain

$$\boldsymbol{\sigma} = \epsilon_0 \sum_l \begin{bmatrix} \frac{b_{lxx}}{k_p - c_l} & \frac{b_{lxx}}{k_p - c_l} & \frac{b_{lxx}}{k_p - c_l} \\ \frac{b_{lxx}}{k_p - c_l} & \frac{b_{lxx}}{k_p - c_l} & \frac{b_{lxx}}{k_p - c_l} \\ \frac{b_{lxx}}{k_p - c_l} & \frac{b_{lxx}}{k_p - c_l} & \frac{b_{lxx}}{k_p - c_l} \end{bmatrix}, \quad (10)$$

where l is summation for s , n and l_n , i.e., $\sum_l =$

$\sum_s \sum_{n=0}^N \sum_{l_n}$. The coefficients are $c_l = p_{l_n} / |\rho_{cs}|$ and

$$\begin{aligned} b_{lxx} &= -2i \frac{\omega_{ps}^2}{\omega_{cs} |\rho_{cs}|} \sum_j b_j \frac{r_{l_n}}{p_{l_n}^2} x_{sj} \frac{n^2}{x_{sj}^2 - n^2}, \\ b_{lxy} &= 2 \frac{\omega_{ps}^2}{\omega_{cs} |\rho_{cs}|} \sum_j b_j r_{l_n} \left[\frac{1}{2} \frac{(n+1)^2}{x_{sj}^2 - (n+1)^2} \right. \\ &\quad \left. - (n \geq 1) \cdot \frac{n^2}{x_{sj}^2 - n^2} + (n \geq 2) \cdot \frac{1}{2} \frac{(n-1)^2}{x_{sj}^2 - (n-1)^2} \right], \\ b_{lxz} &= -2\sqrt{2}i \frac{\omega_{ps}^2}{\omega_{cs} \rho_{cs}} \sum_j b_j c_j \frac{r_{l_n}}{p_{l_n}} \frac{n^2}{x_{sj}^2 - n^2}, \\ b_{lyy} &= -2i \frac{\omega_{ps}^2}{\omega_{cs} |\rho_{cs}|} \sum_j b_j \left\{ \frac{r_{l_n}}{p_{l_n}^2} x_{sj} \frac{n^2}{x_{sj}^2 - n^2} \right. \\ &\quad \left. - \frac{r_{l_n} p_{l_n}^2}{x_{sj}} \left[\frac{(n+1)^2}{x_{sj}^2 - (n+1)^2} - (n \geq 1) \cdot 2 \frac{n^2}{x_{sj}^2 - n^2} \right. \right. \\ &\quad \left. \left. + (n \geq 2) \cdot \frac{(n-1)^2}{x_{sj}^2 - (n-1)^2} \right] \right\}, \\ b_{lyz} &= -2\sqrt{2} \frac{\omega_{ps}^2}{\omega_{cs} \rho_{cs}} \sum_j \frac{b_j c_j}{x_{sj}} r_{l_n} p_{l_n} \left[\frac{1}{2} \frac{(n+1)^2}{x_{sj}^2 - (n+1)^2} \right. \\ &\quad \left. - (n \geq 1) \cdot \frac{n^2}{x_{sj}^2 - n^2} + (n \geq 2) \cdot \frac{1}{2} \frac{(n-1)^2}{x_{sj}^2 - (n-1)^2} \right], \\ b_{lzz} &= -2i \frac{\omega_{ps}^2}{\omega_{cs} |\rho_{cs}|} \sum_j b_j c_j^2 r_{l_n} x_{sj} \frac{[1 + (n \geq 1)]}{x_{sj}^2 - n^2}, \end{aligned}$$

and $b_{lyx} = -b_{lxy}$, $b_{lzx} = b_{lxz}$ and $b_{lyz} = -b_{lyz}$. The matrix form can readily be obtained as

$$\begin{aligned} k_x \delta v_{xl} &= c_l \delta v_{xl} + b_{lxy} \delta E_y + b_{lxz} \delta E_z \\ &\quad + b_{lxx} \frac{1}{\omega} \left(k_z c^2 \delta B_y - \frac{i \sum_{l'} \delta v_{xl'}}{\epsilon_0} \right), \quad (11a) \end{aligned}$$

$$\begin{aligned} k_x \delta v_{yl} &= c_l \delta v_{yl} + b_{lyy} \delta E_y + b_{lyz} \delta E_z \\ &\quad + b_{lyx} \frac{1}{\omega} \left(k_z c^2 \delta B_y - \frac{i \sum_{l'} \delta v_{yl'}}{\epsilon_0} \right), \quad (11b) \end{aligned}$$

$$\begin{aligned} k_x \delta v_{zl} &= c_l \delta v_{zl} + b_{lzy} \delta E_y + b_{lzz} \delta E_z \\ &\quad + b_{lzx} \frac{1}{\omega} \left(k_z c^2 \delta B_y - \frac{i \sum_{l'} \delta v_{zl'}}{\epsilon_0} \right), \quad (11c) \end{aligned}$$

where we have used $\delta J_x = \sum_l \delta v_{xl}$, $\delta J_y = \sum_l \delta v_{yl}$ and $\delta J_z = \sum_l \delta v_{zl}$.

The fluid model is constructed by combining Eqs. (9) and (11). This linear system can be solved as a matrix eigenvalue problem, $k_x \mathbf{X} = \mathbf{M} \cdot \mathbf{X}$, to obtain all solutions of k_x , where the state vector is defined as $\mathbf{X} = [\delta v_{xl}, \delta v_{yl}, \delta v_{zl}, \delta E_y, \delta E_z, \delta B_y, \delta B_z]$. This model has a structure similar to the warm multi-fluid model [16–18] but with significantly larger dimensions and complex-valued coefficients. The matrix dimension is approximately $S \times \sum_n L_n + 4 \simeq S \times N \times (L + N) + 4$, whereas the matrix dimension of the warm multi-fluid model is only $2S + 4$ [16].

For a complex frequency $\omega = \omega_r + i\omega_i$, the dominant mode is typically the one with the largest imaginary part

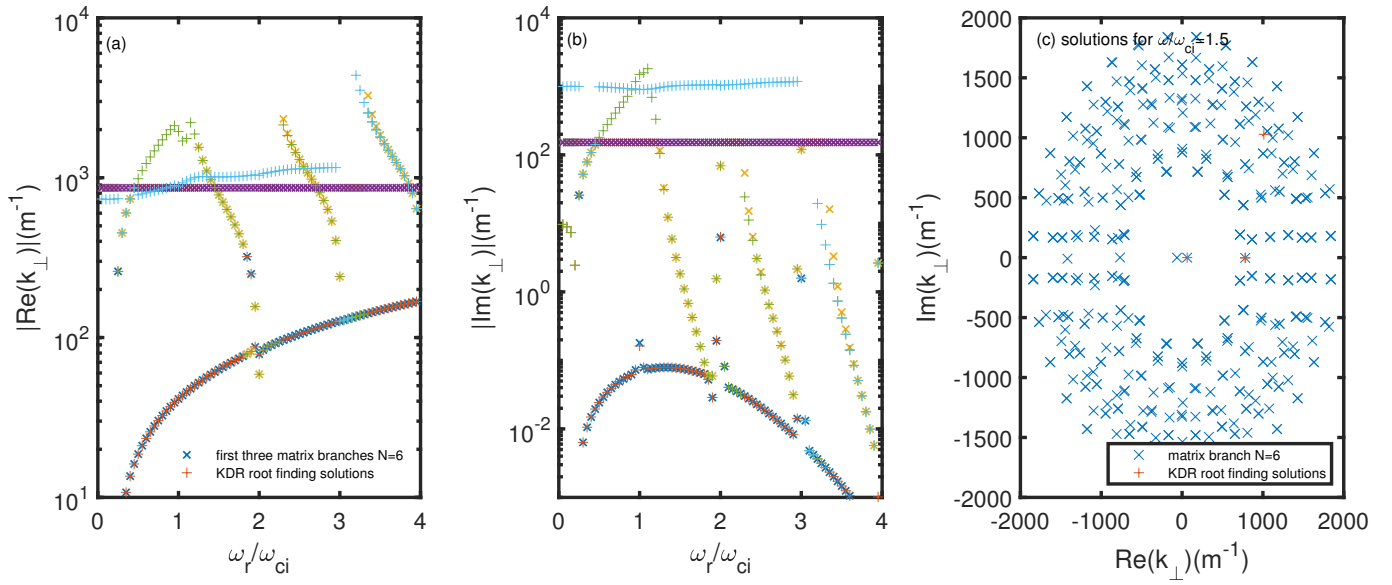


FIG. 2: The comparison of ICW in the fluid matrix system described by Eqs. (9) and (11) with KDR solutions shows excellent agreement for most major solutions, both for the real part $\text{Re}(k_{\perp})$ (a) and the imaginary part $\text{Im}(k_{\perp})$ (b). This indicates that the fluid model can accurately capture ICW fast waves and IBW. More solutions from the fluid matrix are shown in (c) for $\omega_r/\omega_{ci} = 1.5$.

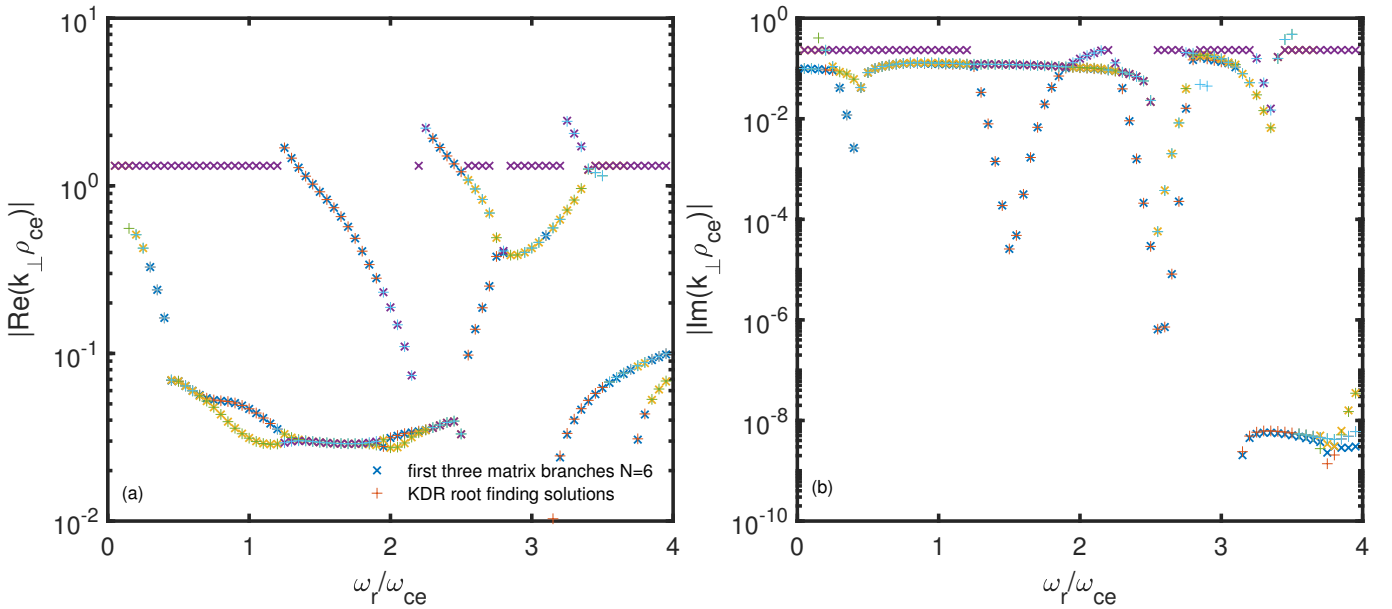


FIG. 3: The comparison of ECW in the fluid matrix system described by Eqs. (9) and (11) with KDR solutions shows good agreement for most major solutions, both for the real part $\text{Re}(k_{\perp})$ (a) and the imaginary part $\text{Im}(k_{\perp})$ (b). This demonstrates that the fluid model can accurately capture ECW O-mode and X-mode waves, as well as EBW.

ω_i . However, for a complex wavenumber $k_x = k_{xr} + ik_{xi}$, the selection criterion differs. We consider the first few solutions with $k_{xr} > 0$ and the smallest $|k_{xi}|$ as the physically relevant solutions. This choice is justified because solutions with large k_{xi} (either rapidly growing or strongly damped) are typically non-physical due to boundary constraints and are unlikely to dominate in realistic scenarios.

To demonstrate the accuracy of this new fluid model, we compare its solutions with those from the KDR in both the ion cyclotron wave (ICW) and electron cyclotron wave (ECW) ranges. This comparison is particularly relevant for plasma wave propagation conditions (i.e., accessibility). The parameters used are taken from Fig. 3 of [10] and Fig. 12 of [17]. Figure 2 presents the ICW solutions, while Figure 3 displays the ECW solu-

tions. The results show that the fluid matrix method agrees well with the KDR solutions for both ion Bernstein waves (IBW) and electron Bernstein waves (EBW), as well as for ICW fast waves (FW) and ECW extraordinary mode (X-mode) and ordinary mode (O-mode). The discrepancies mainly appear in the less important strongly imaginary solutions, which arise from inaccuracies in the fitting of Γ_n for large imaginary components and the truncation of the summation over n to N .

The input parameters for the ICW case are: $S = 2$ (electron and deuterium ion), $B_0 = 6\text{T}$, $n_{s0} = 2e20\text{m}^{-3}$, $T_s = 4\text{keV}$ and $k_z = 10\text{m}^{-1}$, yielding $\rho_{ci} = 0.00152\text{m}$ and $f_{ci} = \omega_{ci}/2\pi = 45.7\text{MHz}$. The input parameters for the ECW case are: $S = 1$ (electron only), $B_0 = 1\text{T}$, $n_{s0} = 6.075e19\text{m}^{-3}$, $T_s = 1\text{keV}$ and $k_z\rho_{ce} = 0.1$, yielding $\rho_{ce} = 7.54e-5\text{m}$ and $f_{ce} = \omega_{ci}/2\pi = 28\text{GHz}$. The small differences in the imaginary part k_{xi} between the ECW O- and X-mode solutions and the KDR results may be due to round-off fitting errors. Since the ratio k_{xi}/k_{xr} is on the order of 10^{-6} , this discrepancy is negligible.

The strong agreement between the fluid model, given

by Eqs. (9) and (11), and the KDR results provides confidence that kinetic effects, such as Bernstein waves, are accurately incorporated into the fluid framework. This could be a crucial step toward developing further applications. For a fixed x , it is also possible to fit $R(x, \lambda)$ directly [8, 14], which would be useful for high-frequency harmonics requiring large N to converge for large λ . However, this approach necessitates refitting each time x changes, which depends on ω , k_z and v_{ts} .

In summary, this work represents the first instance where a fluid model accurately incorporates kinetic Bernstein waves. The fluid matrix method avoids numerical difficulties such as divergence and the need for good initial values when solving the KDR. This approach can be directly applied to ray tracing studies [19], and we anticipate further developments in fast full-wave simulations of ICRF [12, 20] using fluid models with accurate kinetic effects.

The author would like to thank the discussions with Jiahui Zhang and Haojie Ma. The source code for this work is available at <https://github.com/hsxie/fluidbw>.

-
- [1] T. Stix, *Waves in Plasmas*, AIP Press, 1992.
 - [2] M. Brambilla, *Kinetic Theory of Plasma Waves: Homogeneous Plasmas*, Oxford University Press, 1998.
 - [3] H.S. Xie, BO: A unified tool for plasma waves and instabilities analysis, *Comput. Phys. Comm.* 244 (2019) 343-371; Xie, H. S., Denton, R., Zhao, J. S. and Liu, W, BO 2.0: Plasma Wave and Instability Analysis with Enhanced Polarization Calculations arXiv:2103.16014, 2021. <https://github.com/hsxie/bo/>.
 - [4] H. S. Xie, Rapid computation of the plasma dispersion function: Rational and multi-pole approximation, and improved accuracy, *AIP Advances* 14, 075007 (2024).
 - [5] G. W. Hammett and W. F. Perkins, Fluid moment models for Landau damping with application to the ion-temperature-gradient instability, *Phys. Rev. Lett.*, 64, 3019 (1990).
 - [6] G. Hammett, W. Dorland, and F. Perkins, Fluid models of phase mixing, Landau damping, and nonlinear gyrokinetic dynamics, *Phys. Fluids B* 4, 2052 (1992).
 - [7] W. Dorland and G. W. Hammett, Gyrofluid turbulence models with kinetic effects, *Physics of Fluids B* 5, 812 (1993).
 - [8] K. Ronnmark, WHAMP - Waves in Homogeneous Anisotropic Multicomponent Magnetized Plasma, KGI Report No. 179, Sweden, 1982.
 - [9] K. Ronnmark, Computation of the dielectric tensor of a Maxwellian plasma, *Plasma Phys.*, 25 (1983) 699.
 - [10] H. S. Xie and Y. Xiao, PDRK: A General Kinetic Dispersion Relation Solver for Magnetized Plasma, *Plasma Science and Technology*, 18, 2, 97 (2016). Update/bugs fixed at <http://hsxie.me/codes/pdrk/> or <https://github.com/hsxie/pdrk/>.
 - [11] M. Brambilla, *Plasma Phys. Control. Fusion* 41, 1-34 (1999).
 - [12] R. H. S. Budé, D. Van Eester, J. van Dijk, R. J. E. Jaspers and A. B. Smolders, Accelerating simulations of electromagnetic waves in hot, magnetized fusion plasmas, *Plasma Physics and Controlled Fusion*, 63, 3, 035014 (2021).
 - [13] D. Van Eester and E. A. Lerche, Solving the all-FLR ICRH integro-differential wave equation as a high-order differential equation for studying combined ICRH-NBI heating, *Nucl. Fusion* 61 016024 (2021).
 - [14] J. P. M. Schmitt, The magnetoplasma dispersion function: some mathematical properties, *Journal of Plasma Physics*, 12, 1, 51-59 (1974).
 - [15] M. Abramowitz and I. A. Stegun, *Handbook of Mathematical Functions with Formulas, Graphs, and Mathematical Tables*, Dover Publications, 1972.
 - [16] H. S. Xie, H. J. Ma and Y.K. Bai, Plasma wave propagation conditions analysis using the warm multi-fluid model, *Fundamental Plasma Physics* 10 (2024) 100050.
 - [17] H. S. Xie, H. J. Ma and Y.K. Bai, Plasma Waves Accessibility Diagrams: A Tutorial to Include the Fluid and Kinetic Thermal Effects, arXiv: 2111.05669 (2021).
 - [18] H. S. Xie, PDRF: A general dispersion relation solver for magnetized multi-fluid plasma, *Computer Physics Communications*, 185, 670-675 (2014).
 - [19] H. S. Xie, D. Banerjee, Y. K. Bai, H.Y. Zhao and J. C. Li, BORAY: Aray tracing code for various magnetized plasma configurations, *Computer Physics Communications* 276 (2022) 108363.
 - [20] J.H. Zhang, X.J. Zhang, C.M. Qin, W. Zhang and Y.Q. Yang, An alternative method to mimic mode conversion for ion cyclotron resonance heating, *Nucl. Fusion* 64 (2024) 016034.